

# Microbicides for HIV/AIDS. 1. Electrophoretic Fingerprinting the H9 Cell Model System<sup>†</sup>

R. L. Rowell,<sup>\*,#</sup> D. Fairhurst,<sup>‡</sup> S. Key,<sup>§</sup> A. Morfesis,<sup>||</sup> I. M. Monahan,<sup>§</sup>  
M. Mitchnick,<sup>‡</sup> and R. A. Shattock<sup>§</sup>

*Department of Chemistry, University of Massachusetts, Amherst, Massachusetts 01003,  
International Partnership for Microbicides, Silver Spring, Maryland 20910, St. George's  
Hospital Medical School, London SW17 0RE, United Kingdom, and Malvern Instruments Inc.,  
Southborough, Massachusetts 01772*

*Received March 7, 2005. In Final Form: May 7, 2005*

An electrophoretic fingerprint of a CD4+ T-cell (H9) has been produced for the first time. Samples were taken from three separate cultures prepared at different times to obtain a general characterization of the cells. The availability of commercial instrumentation equipped with an auto-titrator has made possible the application of both the 2-dimensional and 3-dimensional representation of electrophoretic fingerprinting. The 2-dimensional treatment has been used to assess the reliability of the data and has detected hysteresis as a possible second-order effect. The 3-dimensional representation has been used to explore the data needed for a reliable overall pattern that characterizes the conditions of pH and conductivity required for an effective microbicide. The dome negative maximum in the electrophoretic fingerprint at high pH, along with the line of zero mobility (LZM) and a dome positive maximum at low pH, are interpreted as evidence for surface carboxyl groups prominent in the alkaline regime and surface amino groups prominent in the acid regime, suggesting that the H9 cell surface is zwitterionic. This has important implications as to the choice and design of microbicide actives.

## Introduction

Worldwide, approximately 40 million people are infected with human immunodeficiency virus (HIV-1).<sup>1</sup> This equates to greater than 1 in every 100 adults on the planet being HIV positive. The epidemic is still growing with over 14 000 new infections each day. Resource-poor nations carry the majority of the disease burden with Sub-Saharan Africa accounting for some 80% of the existing cases. Increasingly, woman and girls are bearing the brunt of the epidemic and, in some locations, now make up the majority of those infected.<sup>2</sup>

The mainstay of modern disease prevention is the preventative vaccine. Unfortunately, developing a preventative HIV-1 vaccine that decisively reduces the rate of spread of the AIDS pandemic is likely to take a number of years, at best.<sup>3</sup> Since the majority of new infections are transmitted through heterosexual contact,<sup>1,4</sup> there is an urgent need to develop alternative measures and technologies to prevent the sexual transmission of HIV. One concept under evaluation is that of a topical microbicide: a vaginally or rectally applied compound designed to inactivate incoming HIV-1 or to prevent the virus from entering or replicating in the cells that it infects, at or near its site of deposition.<sup>5</sup> Only recently, however, has the idea attracted substantial funding and the attention of the research community.<sup>6</sup> Several strategies for micro-

bicide development are being actively pursued. The most developed approaches fall into three broad categories: membrane disruptive agents, charge dependent inhibition of viral attachment/fusion, and the use of anti-retroviral drugs (ARV). The ARVs being considered as microbicides mirror drugs being used in HIV therapy and include nucleoside and nonnucleoside inhibitors of reverse transcriptase. These agents, while highly potent, may also induce resistance. Membrane-disruptive agents, such as Nonoxynol-9, work by destroying the outer envelope layer of the virus, but show little selectivity between virus and cellular membranes. In contrast charge-dependent viral inhibition is an appealing strategy in that the virus is "stopped" in the vaginal lumen prior to entry into the host's cells. A variety of polyanions have been developed for this application,<sup>7-9</sup> and they have the advantages of being cheap to produce and highly biocompatible.

HIV has been extensively studied in terms of its genetic content, biological activity, and reactivity of its surface constituents. The amino acid sequence and tertiary structure of gp120 for instance is well-known and is the basis for much of today's HIV vaccine and therapeutic drug development efforts. However, there have been relatively few studies of HIV as a particle with bulk surface characteristics dictated by specific surface moieties. Historically, this type of research is carried out on inert, inorganic particles, most often in industrial/material science applications. Of equal importance to the surface characteristics of the virion are the surface characteristics of HIV's target cells, the cells that HIV initially infects. Whatever properties exist on HIV, receptive conditions must also exist on the target cells to enable physical contact: a prerequisite to infection. CD4+ T-cells are the primary target cells for HIV.

<sup>†</sup> Part of the Bob Rowell Festschrift special issue.

\* To whom correspondence should be addressed.

# University of Massachusetts.

‡ International Partnership for Microbicides.

§ St. George's Hospital Medical School.

|| Malvern Instruments Inc.

(1) UNAIDS, *AIDS Epidemic update 2004*, Geneva, 2004.

(2) Ojikutu B. O.; Stone, V. E. *N Engl. J. Med.* **2005**, *352*, 649.

(3) Moore, J. P. *N. Engl. J. Med.* **2005**, *298*.

(4) Evans, A.; Lee, R.; Mammem-Tobin, A.; Piyadigamage, A.; Shann, S.; Waugh, M. *SKINmed* **2004**, *3*(3), 149.

(5) Stone, A. B.; Hitchcock, P. J. *AIDS* **1994**, *8*, 285.

(6) Shattock, R. A.; Moore, J. P. *Nat. Rev. Microbiol.* **2003**, *1*, 25.

(7) D'Cruz, O. J.; Uckun, F. M. *Curr. Pharm. Des.* **2004**, *10*, 315.

(8) Turpin, J. A. *Expert Opin. Investig. Drugs* **2002**, *11*, 1077.

(9) Neurath, A. R.; Strick, N.; Li, Y. Y.; Debnath, A. K. *BMC Infect. Dis.* **2001**, *1*, 17.

Polyanion microbicides are based on the premise that they are able to bind to a sterically restricted surface on the viral envelope glycoprotein that has a basic charge.<sup>10,11</sup> If virus–cell interaction is inhibited, then HIV-1 is prevented from entering cells and it becomes, effectively, an inert particle. Since the interaction is “charge related”, one new paradigm for the selection or design of antimicrobial compounds or compositions is to assess their ability to affect the surface chemical properties of the target cell or virus. We propose that the target cell and virus can be considered as particles whose surface physicochemical properties can be evaluated using simple, well-established techniques such as zeta potential (or the actual measured quantity, the electrophoretic mobility). Accordingly, a program of study has been initiated, by the International Partnership for Microbicides, at St. George’s Hospital Medical School, to characterize the zeta potential of HIV-1 virus over a range of conditions relevant for microbial infection, in particular encompassing those typical of the vaginal environment pre- and post-intercourse. The aim of our work is to obtain direct experimental evidence of the properties of the AIDS virion in situ before, during, and after interaction with microbicides. We are also looking to similarly characterize the target cells. This ambitious and long-term project is underway, and in the present work, we report the first studies of the properties of a model system, namely human CD4+ H9 cells. Studies are concurrently being undertaken on two other human CD4+ T-cell lines used for in vitro culture of HIV-1, viz C8166 and Molt-4. The results of these studies will be the subject of a separate paper.

It has long been recognized that surface chemical properties play an important role in the behavior of microorganisms and that gene expression may be modified by responses of the surface to changes in environment.<sup>12</sup> The measurement of the electrokinetic properties of red blood cells have been very extensively studied and reviewed.<sup>13</sup> However, very little published work exists on the electrokinetic profile of T-cells, and the precision of previous published electrokinetic data on biological surfaces has been limited by the nature of the instrumental technique used. The present work represents, for the first time, studies of the dynamic electrical properties of the biological surface of human CD4+ T cells (H9). The advent of phase analysis light scattering (PALS)<sup>14</sup> and the development of a commercial instrument based on the technique<sup>15</sup> have removed the severe difficulties in obtaining reliable data in physiological environments.

The contour diagram patterns we obtain directly in our work by the nondestructive measurements of particle microelectrophoresis on colloidal particulate systems, resemble a human fingerprint pattern. So we can define the electrophoretic fingerprint (EF) as the representation of the measured particle electrophoretic mobility as a function of the two characteristic variables: pH and  $p\lambda$ , the logarithm of the specific conductance (where  $\lambda$  is

expressed in units of  $\mu\text{S cm}^{-1}$ ). For deionized, double distilled water,  $p\lambda$  is approximately 0.3 so that our reference solvent has a  $p\lambda$  close to zero; and a logarithmic scale from 1 to 5 covers nearly all of the solution conditions of current interest. It is important that both the scales be logarithmic in character because the driving force for chemical change is the free energy, or chemical potential, and the theory is based on a logarithmic scale of the activity.

We need, however, to distinguish our definition from the more widely known one used in DNA analysis in which the EF is the chromatogram or electrophoretogram obtained by cleaving a protein by enzymatic action and subjecting the resulting collection of peptides to two-dimensional chromatography or electrophoresis. Our work is based on the techniques of particle microelectrophoresis, which is clearly a different methodology from DNA fingerprinting. However, DNA fingerprinting has been around longer and the confusion has crept into the literature. For example, there are two definitions for the word “fingerprinting” in Webster’s New Collegiate Dictionary, 1980 edition; the first refers to the human fingerprint, the image of which we use as the basis for EF, and the second is the description of DNA fingerprinting we have just quoted. Currently, a search of the scientific literature on “fingerprinting” results in numerous references to DNA fingerprinting but very few on EF.

An important feature of our approach is that the measured electrophoretic mobility is assumed to be a function of the colloidal microstate of the system that is represented by the characteristic (microstate) variables pH and  $p\lambda$ . The variable pH is not an independent variable since a change in pH also changes the conductivity of the system. The variable  $p\lambda$  can be increased by the addition of salt or other electrolyte and can be decreased by the dilution of the system with water. In most, if not all, practical instances,  $p\lambda$  can be regarded as an independent variable. The variables pH and  $p\lambda$  taken together constitute the principal microstate variables since other variables, such as temperature, pressure, and the concentration of the colloidal material, are kept constant. In this first treatment of the problem, we have attempted to keep the concentration of the colloid (the H9 cells) constant and held as close as possible to that of the growth medium from which the experimental aliquot was withdrawn. In future work, and in a more general application of the EF technique, we will study more carefully both the particle size distribution and the number concentration of the colloidal particles.

The EF technique was first applied to latex surfaces.<sup>16</sup> Rowell et al. have published many papers on the subject; the most recent understandings have been reviewed and summarized.<sup>17</sup> However, in all of the surfaces studied to date, there have been no attempts to remove an aliquot of growing cells from the growth media and resuspend the cells, still living, in an apparatus where direct measurements of pH,  $p\lambda$ , and the electrophoretic mobility are obtained. The University of Rostock group has also developed the concept of EF in the study of human body fluids for the treatment of a variety of pathological conditions.<sup>18,19</sup> In our work, we apply the EF technique,

(10) S. Shaunak, Thornton, M.; Teo, I.; Chandler, B.; Jones, M.; Steel, S. *J. Drug Targeting* **2003**, *11*, 443.

(11) Moulard, M.; Lortat-Jacob, H.; Mondor, I.; Roca, G.; Wyatt, R.; Sodroski, J.; Zhao, L.; Olson, W.; Kwong, P. D.; Sattentau, Q. J. *J. Virol.* **2000**, *74*, 1948.

(12) Richmond, D. V.; Fisher, D. J. *Adv. Microbial Physiology* **1973**, *9*, 1.

(13) Seaman, G. V. F. In *The Red Blood Cell*; Surgenor, D., Ed.; Academic Press: New York, 1975; Vol. II, Chapter 27.

(14) Miller, J. F.; Schatzel, K.; Vincent, B. J. *Colloid Interface Sci.* **1991**, *143*, 532.

(15) Tschamuter, W. W.; McNeil-Watson, F.; Fairhurst, D. In *Particle Size Distribution III: Assessment and Characterization*; Provder, T., Ed.; ACS Symposium Series 693; American Chemical Society Washington, DC, 1998; Chapter 22.

(16) Morfesis, A. Ph.D. Thesis, University of Massachusetts, 1986.

(17) Rowell, R. L.; Yezek, L. P.; Bishop, R. J. In *Particle Sizing and Characterization*; Provder, T., Texter, J., Eds.; ACS Symposium Series; American Chemical Society: Washington, DC, 2004; Vol. 881, p 201. Yezek, L.; Rowell, R. L. *Langmuir* **2000**, *16*, 5365.

(18) Knippel, E.; Budde in “Interfacial Electrokinetics and Electrophoresis”, *A. Surfactant Science Series* **2002**, *106*, 693.

(19) Donath, E.; Walther, D.; Shilov, V. N.; Knippel, E.; Budde, A.; Lowack, K.; Helm, C. A.; Moehwald, H. *Langmuir* **1997**, *13*, 5294.

for the first time, to the study of a living moiety. The EF can be represented either as a contour diagram or as a wireframe, in 2- or 3-dimensions, respectively. A sister technique, hydrodynamic fingerprinting (HF),<sup>20</sup> will be applied in the future studies of cells and viruses.

### Experimental Section

**Samples.** H9 cells are a human cutaneous CD4+ T-cell lymphoma derived from the HUT78 cell line, which is particularly permissive for HIV-1 replication.<sup>21</sup> Most laboratory T-cell lines express only CXCR4 receptors and are, therefore, only susceptible to X4 strains of HIV-1. This leads to these strains of HIV-1 being called T-tropic, syncytial-inducing virus. H9, C8166, and Molt-4 cells are all capable of supporting both the infection and replication of these strains of HIV.

**Preparation of the Samples.**<sup>22</sup> Tissue culture work was carried out under aseptic conditions in a Class II biological safety cabinet. H9 cells were maintained in RPMI growth medium supplemented with 10% heat inactivated fetal calf serum, 2mM glutamine, 100 i.u./mL penicillin and 100  $\mu$ g/mL streptomycin at 37 °C in a humidified 5% CO<sub>2</sub> incubator. The cells were routinely maintained every 3–4 days in 75 cm<sup>3</sup> filter cap tissue culture flasks by removing 4 mL of cells and adding them to 16 mL of fresh growth medium.

Prior to electrophoretic analysis, 10 mL aliquots of H9 cells were spun at 1000 rpm for 5 min and the pellets resuspended in 10 mL volumes of the appropriate NaCl concentrations under examination (1, 5, 10, 50, 100, 154, and 200 mM). Samples were also examined in distilled water. The range of ionic strengths was extended below that of usual physiological conditions in order to be able to more completely develop the EF. The range of pH values was chosen to cover that known for fluids found in the lower female reproductive tract, including vaginal fluid and semen.<sup>23,24</sup>

**Instrumentation.** Electrophoretic mobility (zeta potential) measurements were made using a Malvern *ZetaSizer NanoZS* operating in the fast field reversal mode (PALS) equipped with an MPT-2 automatic titrator. The addition of the auto-titrator was found to dramatically improve the rate of data acquisition. This system has unique capabilities because it can be set up to titrate up to 100 points between the ranges of pH 1 to pH 13 starting with a minimum sample volume for this case of 5.5 mL. The titrator can be set up to use three titrants at a time. This can include the same same titrant at different concentrations, for example 0.25 M HCl and 0.01 M HCl. This allows the titration to be measured with an addition of minimum volume of titrants at the extremes of pH and accurate adjustment of pH close to pH 7. The titrants are introduced during the measurements via displacement type syringes. One stroke of the piston is 84  $\mu$ L in 300 steps, each of 0.28  $\mu$ L. The valves directing the titrants are low dead volume valves, specifically designed for these types of applications.

**Data Analysis.** The directly measured quantities were the pH, the conductivity ( $\rho$ ) and the electrophoretic mobility ( $U_{em}$ ). The zeta-potential (in units of mV) may be obtained by multiplying the reported mobilities by the constant 12.68; the assumption that the Smoluchowski equation applies<sup>25</sup> is not unreasonable given the size of H9 T-cells and the solution ionic strength. EXCEL files were prepared for all three variables in a format suitable for data analysis using proprietary software algorithms, SURFER<sup>26</sup> and two types of analyses were carried out. Since each run was carried out over a very narrow range of conductivity, it was possible to obtain a 2-dimensional, statistically obtained,

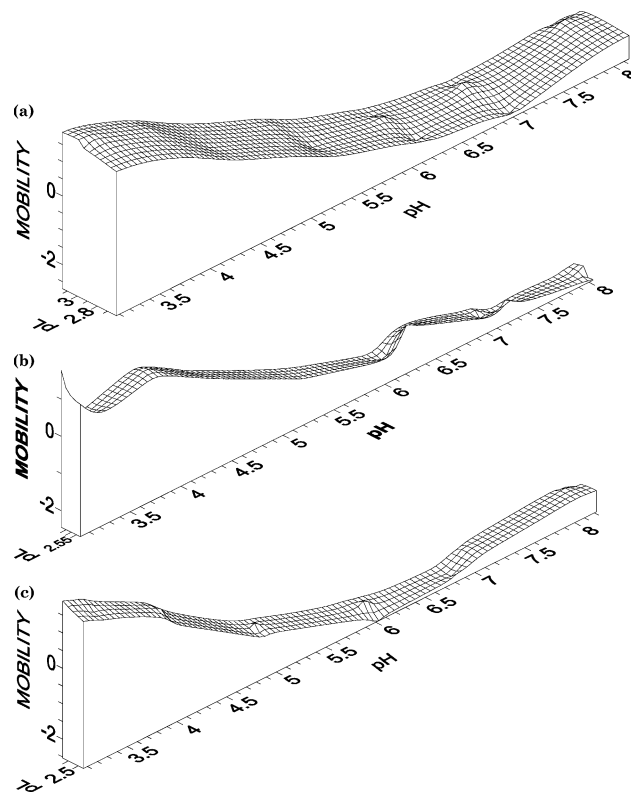


**Figure 1.** (a) Wireframes for H9 cells: Run L in 1 mM NaCl; pH sweep 3.17–8.15–3.07. Day 4. (b) Wireframes for H9 cells: Run P in distilled water; pH sweep 3.01–8.04–3.1. Day 1. (c). Wireframes for H9 cells: Run R in distilled water; pH sweep 3.25–8.22–3.06. Day 3.

profile of  $U_{em}$  as a function of pH at approximately constant  $\rho$  using the wireframe methodology in the SURFER program. This approach is the first use of the 2-dimensional profile to examine the dynamics on a growing cell system but it is reminiscent of the early work on EF where electrophoretic mobility distributions were used in the work on the use of latex particles as biological indicators.<sup>27</sup>

The wireframes were a useful indicator of the reproducibility of the data at a particular salt concentration and also indicated the effects of sample age and measurement protocol that need to be explored in further work.

All of the data used to generate the wireframes were also assembled in various files to prepare electrophoretic fingerprints both in the contour form and in a 3-dimensional wireframe form using SURFER as discussed below.

### Results and Discussion

The general approach to our analysis is to proceed through two stages. In the first stage, which involves presentation and discussion of Figures 1–3, we employ the two-dimensional form of electrophoretic fingerprinting using wireframes generated by the program SURFER. Wireframes are statistical representations of the data at approximately constant  $\rho$ ; this experimental condition is readily achievable through use of the automatic titration capability of the Malvern NanoSizerZS. This feature is especially important at low  $\rho$  where a change in pH results in a measurable change in conductivity that, in turn, leads to curvature in pH– $\rho$  space. Such an effect has been demonstrated previously.<sup>17</sup> The wireframes serve to exhibit both the statistical reliability of the data and also to display visibly the effects of hysteresis. By this we mean that the upscale and reverse downscale parts of the experimental measurement regime do not exactly coincide.

(20) Prescott, J. H.; Shiau, S.-J.; Rowell, R. L. *Langmuir* **1993**, *9*, 2071–2076.

(21) Popovic, M.; Sarngadharan, M. G.; Read, E.; Gallo, R. C. *Science* **1984**, *224*, 497.

(22) Portions of the Sample preparation and Instrumentation sections are from the thesis of Suzie Key, BSc Biomedical Sciences, St George's Hospital Medical School, London 2004.

(23) Katz, D. F.; Anderson, M. H.; Owen, D. H.; Plenys, A. M.; Walmer, D. K. In *Vaginal Microbicide Formulations Workshop*; Rencher, W. F., Ed.; Lippincott-Raven Publishers: Philadelphia, 1998.

(24) Katz, D. F.; Owen, D. H. *Contraception* **1999**, *59*, 91.

(25) Shaw, D. J. *Electrophoresis*; Academic Press: London, 1969.

(26) Golden Software, Inc.: Golden, CO.

(27) Marlow, B. J.; Fairhurst, D.; Schutt, W. *Langmuir* **1988**, *4*, 776.

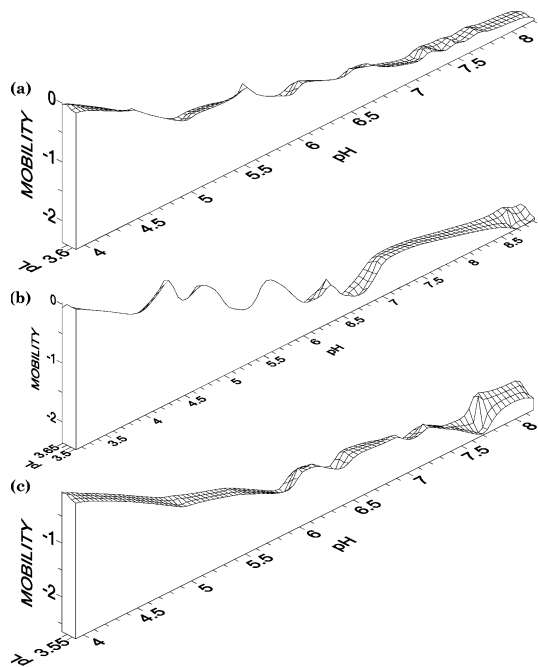


**Figure 2.** (a) Wireframes for H9 cells: Run B in 10 mM NaCl; pH sweep 5.5–8.2–3.9 Day 2. (b) Wireframes for H9 cells: Run X in 10 mM NaCl; pH sweep 4.3–8.9–3.1. Day 3. (c) Wireframes for H9 cells: Run A in 10 mM NaCl; pH sweep 6.0–8.2–3.9. Day 2.

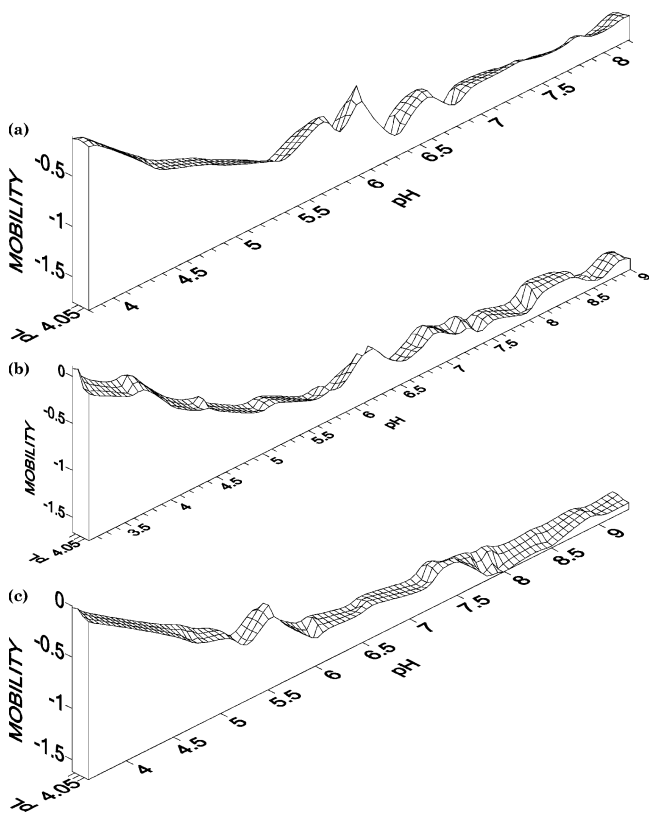


**Figure 3.** (a) Wireframes for H9 cells: Run C in 100 mM NaCl; pH sweep 5.7–8.2–3.8. Day 2. (b) Wireframes for H9 cells: Run W in 100 mM NaCl; pH sweep 6.1–9.0–3.1. Day 3. (c) Wireframes for H9 cells; Run D in 100 mM NaCl: pH sweep 5.2–3.6–9.3–6.0. Day 4.

Both the upscale and downscale pH protocols are indicated on the individual wireframe plots. The resulting curve is not smooth but exhibits bumps and cusps. We made no attempt to smooth the data; the irregularities encountered will be useful in further studies when we will try to

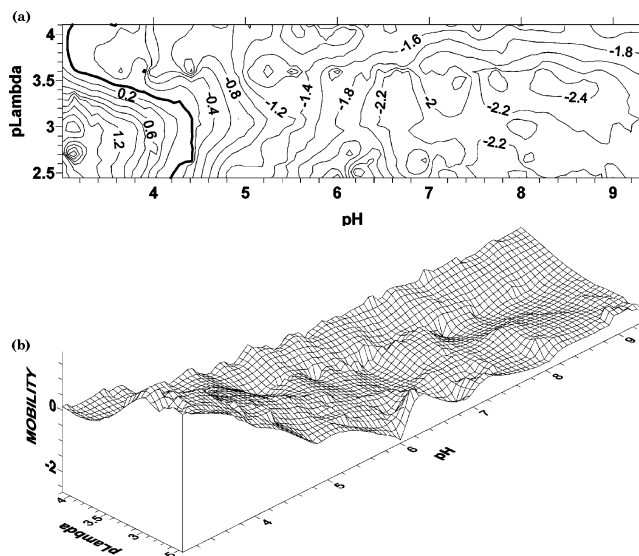


**Figure 4.** (a) EF contour map of H9 cells prepared from the data of Figures 1–3. The LZM is shown in bold. (b) EF wireframe map of H9 cells prepared from the data of Figures 1–3.

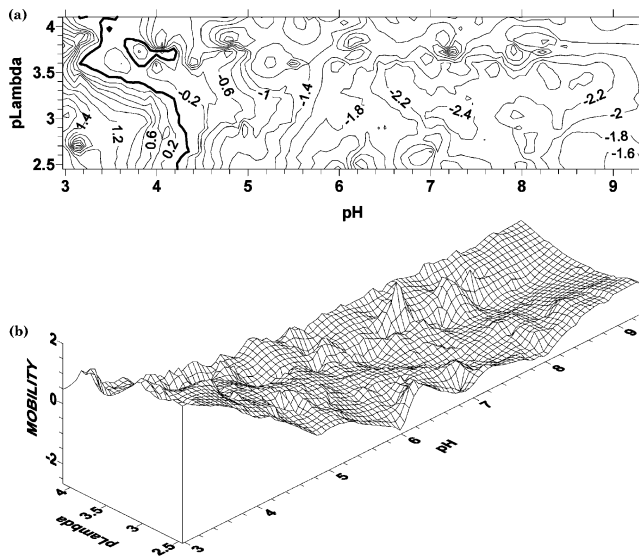


**Figure 5.** (a) EF contour map prepared from the data of Figure 4; with the addition of runs M, N, and O at 5mM NaCl and runs I, J, and K at 50 mM NaCl. The LZM is shown in bold. (b) The EF wireframe map corresponding to Figure 5a.

determine their exact cause. It is useful to remember that we are, in this initial study, examining living, growing systems that have been subjected to minimum treatment without extensive washing or ultrafiltration. This was to ensure that the system remains in a state that is as close as possible to that of the growth medium from which the aliquot was drawn. A second problem pertains to the state of the system equilibrium. The system is not static; rather we are dealing with measurements on aliquots taken from a dynamic, growing system. Further studies are necessary to understand both the equilibration time in the bulk growth medium and the equilibration time in the measurements made on the aliquot drawn. In summary, the first stage is the wireframe analysis (a 2-dimensional fingerprint) to explore the general properties of the data in pH– $p\lambda$  space.

In the second stage of our analysis, given in Figures 4–6, we use the wireframe data in a systematic manner to display: first, the overall dependence of the data in pH– $p\lambda$  space by obtaining the first approximation to the

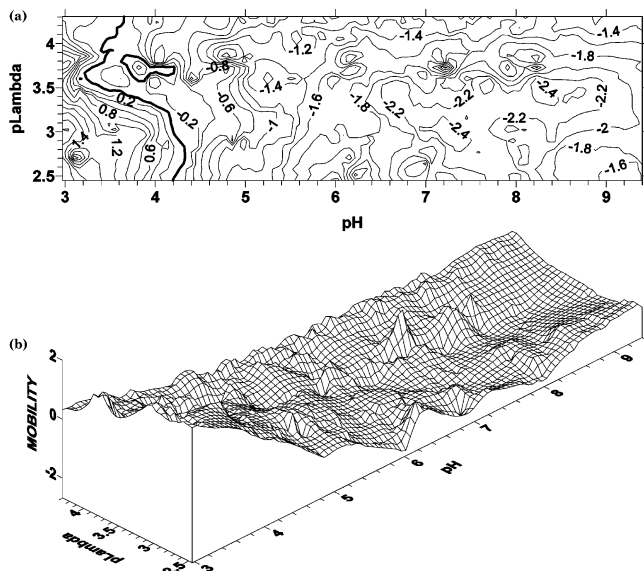


**Figure 6.** (a) EF contour map of H9 cells extended to the higher salt regime by inclusions of runs V and F at 154 mM NaCl and runs G, T, and U at 200 mM NaCl. The LZM is in bold. (b) EF wireframe map of H9 cells corresponding to Figure 6a.

electrophoretic fingerprint, i.e., the three-dimensional EF. Then we continue in Figures 5 and 6, filling in more of the data, to obtain the most complete fingerprint possible with all of the experimental data collected. In summary, the second stage of the analysis displays the effect of adding more data and in the present results demonstrates that the main features of the contour form of the EF remain essentially unchanged.

Beginning then with Figure 1, we show wireframes constructed for the lowest salt concentration studied. The actual particle concentrations were not measured but were kept constant, as determined by the biopreparation. In further work, we will examine the effects of particle (cell) concentration. Run L was carried out in an environment of 1mM aqueous NaCl from a sample taken at day 4 from the growth media. The effects of sampling time seem to be second-order to the establishment of a characteristic fingerprint of the system, but this is an effect to be examined in subsequent work. Another second-order effect is the measurement protocol or pH path pursued. For example, in run L, the measurement started at pH 3.17, then advanced upscale to pH 8.15, and then downscale to return to pH 3.07. There is evidence from this and other runs that the pH path followed may have significant hysteresis effects. Preliminary data has indicated that pH cycling does not result in cell death, at least over the time scale of our experiments. This aspect is being pursued further in more detail because of its implications to biological activity. For the three runs in Figure 1, the day of sampling and the pH protocol followed are indicated in the legend. We generally followed the same procedure in all of the data reported, but exceptions are noted as the results are discussed below. Runs P and R were carried out by dispersing the sample in distilled water. It is clear that even the small sample contributed significant electrolyte to the previously pure water as evidenced by the subsequent  $p\lambda$  level of 2.5. This is an order of magnitude higher than the  $p\lambda$  range of 0.8–1.2 found with similar procedures in latex and oxide systems that had reached  $\text{CO}_2$  equilibration with the laboratory atmosphere.<sup>17</sup> For reference, the specific conductance of 1 mM aqueous NaCl at 25 °C is 123.7  $\mu\text{S}/\text{cm}$  giving a  $p\lambda$  of 2.09. The difference in the electrolyte environment is also shown by the broader

range of  $p\lambda$  found in the 1 mM NaCl solution, run L, compared to runs P and R in distilled water. Run L also occurs at a slightly higher value of  $p\lambda$ . The differences in the profiles for runs P and R could easily result from a few outlier points since the SURFER program fits all of the data and is extremely sensitive to small variations. We have not yet developed a criterion for rejecting points and, in the present analysis, have not averaged the data. Run P consisted of 11 sets of 6 points at each of 11 pH values, whereas run R consisted of 12 sets of 6 points at each of the 12 pH values. Hysteresis considerations appear to explain the differences in the profiles observed, but this has to be confirmed.

Figure 1 contains data for two different values of  $p\lambda$ : 1 mM and water. All of the other figures are for a single value of  $p\lambda$  (e.g., 10 and 100 mM). So run L strictly cannot really be compared to runs P and R. However, the profiles of all three runs are similar and within the range of experimental error; hence, we included all three in the subsequent preparation of Figures 4–6.

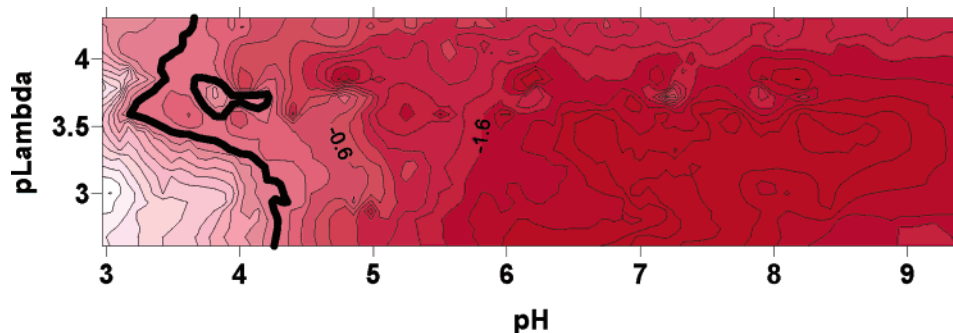
In Figure 2 are shown wireframes for three replicate runs of the H9 cells in 10 mM NaCl. The three runs have been collected at very nearly constant conductivity with a  $p\lambda$  of 3.6. The pH protocols were of the same type as in Figure 1, but the extrema points differed so that one has to mentally shift the axes to compare the profiles. This is taken care of in the EF that is produced in Figure 4 because, there, the EF is referenced to points in  $\text{pH}-p\lambda$  space. Because this is the first time that the SURFER data analysis algorithms have been applied to a dynamic, living system, we have followed the most objective analysis possible produced by the software program. During the analysis, it is possible to stretch the axes, and thus modify the scales, to make comparison of the figures easier. In the present work, we have chosen to accept the statistical results and maps without distortion.

Figure 3 shows wireframes for three replicate runs of the H9 cells in 100 mM NaCl. There are significant ripples in the profiles of the different runs, but we note that both the sample day and the pH profiles differ. This suggests that there is more to be learned about the dynamics and reproducibility of the biopreparation. Nevertheless, the raw data of Figure 3 were examined, in more detail, to see if there might be some other simpler reason for the irregularities. Run C consisted of 3 measurements at each of the 16 pH values, whereas W comprised 3 measurements at 18 pH values, and D was 3 measurements at 16 pH values. However, the cusp and dip observed, for example between pH 6 and pH 6.3 in run C, seemed to arise because at pH 6.05 three mobility values of  $-0.84$ ,  $-1.1$ , and  $-1.2$  were obtained, whereas at pH 6.36, the mobilities were  $-1.74$ ,  $-1.42$ , and  $-1.53$ . Therefore, over a span of only 0.28 pH units, the statistical analysis algorithm had to accommodate a low value of  $-0.84$  and a high value of  $-1.74$ ; this is more than a factor of 2. Clearly, we need to learn and understand more about what causes the fluctuations in the data.

Notwithstanding the significant differences in the wireframe scans of Figures 1–3, the EF prepared from an analysis of all of the data points, as shown in Figure 4 gives a not unreasonable surface. The EF is represented in contour form in Figure 4a and in 3-D wireframe form in Figure 4b. In all, a total of 509 data points were used.

Three significant features of the EF are apparent from inspection of Figure 4, and these are also seen in Figures 5 and 6 where significantly more experimental data was included:

(1) A line of zero mobility (LZM) that traces an s-shaped curve in the pH 3 to 4 region. The LZM follows a canyon



**Figure 7.** EF Contour map of H9 cells with the same data of Figure 6, except that the runs P and R, the distilled water runs, were removed and a color scale has been added; red for negative mobilities and tones to pink at zero mobility then bleaches to white or blank at maximum positive mobility. The LZM is in bold to emphasize the demarcation between positive and negative surface charge.

wall as opposed to a valley in pH– $p\lambda$  space since the mobility develops a sharp positive maximum at lower pH and a broad negative maximum at higher pH.

(2) The low-pH positive maximum that appears at a solution condition of about pH 3 and  $p\lambda$  2.8.

(3) The third feature is the location of the negative maximum which appears to be around pH 8.5,  $p\lambda$  3.4.

Given that the surface of a biological moiety would be expected to be reminiscent of that of a protein (containing carboxyl and amino groups), the broad alkaline pH maximum is of the type observed in earlier work on a carboxyl-amidine, zwitterionic polymer latex.<sup>17</sup> In that system, there was also an LZM and an increasing positive mobility at low pH. However, the specific features were quite different: a maximum negative mobility of  $-6.0$  and a positive mobility around  $+2.0$ . Also, the path followed by the LZM was totally different.

In Figure 5, we show an intensified EF where additional data has been included by the addition of three runs of H9 cells dispersed in 5 mM NaCl (runs M, N, and O) and three runs of H9 cells dispersed in 50 mM NaCl (runs I, J, and K). The inclusion of the 50 mM runs caused a small shift in the LZM arising from additional data. The pattern becomes complicated in the region around pH 3.9,  $p\lambda$  3.7 as shown by the unusual feature of a circular LZM. This is certainly a curiosity and may simply be a way of representing a plateau of near-zero mobility. The position of the peak of the broad negative maxima at high pH becomes less distinct.

In Figure 6, we have extended the EF to the highest electrolyte region by inclusion of runs F and V at 154 mM NaCl and runs G, T, and U at 200 mM NaCl. The shift of the LZM toward higher pH is confirmed by the additional data. The exact location of the broad negative pH maxima in the alkaline region becomes less clear but might be expressed as occurring at a solution condition of  $p\lambda$  3.3 and pH over the decade range 7.3–8.3. Since the uncertainty of the electrophoretic mobility measurement is in the first decimal place, a more precise definition is beyond the precision of the data. The implication of the inclusion of the additional data points is that the protocol and distribution of data points have small effects on the details of the contour pattern obtained. The broad features are the same but the detailed pattern is not insignificant.

Finally, in Figure 7 we show the contour representation of the data in Figure 6, except that the two distilled water runs (P and R) have been removed. In addition, the variation in mobility is emphasized by a red-shading that is most intense for negative values of mobility; the tone decreases smoothly to white/blank for the highest positive mobility value. It is noted that all of the mobility values to the left of the LZM are positive; the contour interval

is 0.2 so that the highest positive mobility contour line shown is  $+1.8$ . Clearly, the removal of the two distilled water runs makes very little difference in the contour-line pattern in support of our assumption made in the discussion of Figure 1.

There are four principal features in the final result, i.e., the EF of Figure 6, or Figure 7. Of special significance is the fact that the maxima in the mobility are caused primarily by the relaxation effect as shown in earlier work<sup>17</sup> and can be attributed to the extensive ionization cloud around strongly ionized surface functional groups. The summary is as follows:

**1. Alkaline Maximum.** The negatively charged alkaline maximum has a narrow dome around  $p\lambda$  3.3 and extending over a range in pH from 7.3 to 8.5. This seems to be characteristic of a surface carboxyl group as judged from a comparison with the results of published work using a variety of latex polymer colloid systems.<sup>17</sup> It should be noted that the H9 cell, although used as a model system, is cultured in a chemically complex aqueous milieu and cannot be purified and cleaned to the same extent as model polymer colloids.

**2. Acid Maximum.** The positively charged acid maximum around pH 3.1,  $p\lambda$  2.7 is very nearly the same as that observed for the aqueous titanium dioxide system.<sup>17</sup> For  $\text{TiO}_2$ , that feature appeared to arise from protonation of a surface oxygen group. In the present case, however, the pattern of the LZM is more consistent with protonation of an amino group in the acid regime. Therefore, the sharp positive maximum here is likely due to protonated nitrogen. Moreover, the exact locus of the feature may depend on the nature of the electrolyte used as evidenced by the different effects seen with NaCl, KCl,  $\text{NaNO}_3$ , and  $\text{KNO}_3$  on  $\text{TiO}_2$ .<sup>17</sup> More data is needed to map the solution region of interest in greater detail. Unfortunately, experimental measurements are very difficult in this region since it is very close to the edge of the experimentally inaccessible region.<sup>17</sup>

**3. Line of Zero Mobility (LZM).** The position and meandering of the LZM in pH– $p\lambda$  space is similar to that observed in an amidine-carboxyl zwitterionic system.<sup>17</sup> It is definitely quite different from the LZM found for aqueous titanium dioxide, that exhibits only a small change in  $p\lambda$  within a narrow range in pH above pH 6 and is dependent also on the exact nature of the salt used. Since the surface of H9 cells are proteins, the positive peak is likely to arise from protonated amino groups.

**4. LZM Loop at pH 3.8,  $p\lambda$  3.7.** This feature arises from the statistical analysis of the SURFER program and could be regarded as an artifact since the data are limited in that region. A more plausible interpretation is that in that region, the LZM opens up into a plateau of

zero mobility so that the colloid is neutral in charge over a small region in  $\text{pH}-\text{p}\lambda$  space.

### Summary and Conclusions

First, we wish to re-iterate that this is a work-in-progress and the current data has, not unexpectedly, raised a number of issues that need to be resolved.

Importantly, for the first time, the electrophoretic fingerprinting (EF) methodology has been applied to a living system, i.e., measurements on cell aliquots taken from biomedica in which human CD4+ H9 cells were growing.

Measurements have been carried out over a broad range of  $\text{pH}$  and  $\text{p}\lambda$ . This has allowed a quantitative in situ representation of the variations in electrophoretic mobility (and, thereby, surface charge) that occur as a result of changes in the ionic strength of the system from added salt and changes in  $\text{pH}$ . Classical electrophoretic measurements on inorganic and polymer colloid systems have usually been carried out at relatively low ionic strength whereas systems of biological interest are, of necessity, at physiological saline conditions (154 mM NaCl) or at much higher ionic strength ( $>200$  mM) more or less according to the details of the application involved, such as those in vaginal fluids and semen.

We have found that 2-dimensional EF is a useful tool to obtain a rapid display of the effect of preparatory and environmental variables on the system, i.e., the effects of time, state of cell growth,  $\text{pH}$ , salt concentration, and other additives of interest. The 2-dimensional EF scan can also be used to test for, and to explore the effects of hysteresis in the system. The 2-dimensional EF scan can also provide a rapid comparison of replicate measurements to look for reproducibility and/or time-dependent effects through automatic statistical analysis of the data using the SURFER program.

An overview of the surface electrical state of a colloidal system can be obtained in the first approximation by as little as three 2-dimensional EF scans taken at low, medium, and high salt concentration (such as was obtained in Figure 4) and combined using the 3-dimensional EF approach to provide a visual representation both as a contour diagram and as a 3-dimensional wireframe plot.

The initial survey at low, medium, and high salt concentration provides a guide to further fruitful areas to study which may include the entire or extended  $\text{pH}-\text{p}\lambda$  domain or selected regions according to the information desired. Equilibration time, the protocol design and distribution of data points, colloid number concentration, and particle size distribution along with the practical goals described below are areas to prioritize in future research.

The CD4+ H9 cell system has been explored in some detail over the  $\text{pH}$  range from 3 to 9.4 and conductivity,  $\text{p}\lambda$  from 2.5 to 4.3. Upon dispersion in distilled water, the

system liberates considerable electrolyte so that the minimum experimental  $\text{p}\lambda$  is about 1 order of magnitude above that found with cleaned polymer latex systems. Figure 1 showed that the 2-dimensional wireframe for 1mM H9 cells was closely similar to that in pure water but cell-viability and the apparent liberation of electrolyte needs to be examined further to see if it makes any difference from a practical (biological activity) or physicochemical (effect on the measurements) sense.

Four features of the EF of H9 cells have been discussed to suggest the nature of the surface chemistry of the system. The four features are as follows: (1) the negatively charged alkaline maximum; (2) The positively charged acid maximum; (3) The LZM or line of zero mobility; (4) The LZM loop or plateau of zero mobility.

The ultimate goal is to study HIV itself as well as the microbicides for interaction with the virus. Work on the model (T-cell) systems will provide a better understanding of the effects of solution  $\text{pH}$  and conductivity that can be extended to HIV. This is crucial since the actual conductivity in the vaginal tract can vary enormously depending on the health of the epithelial tissue, time of month, use of vaginal preparations, intercourse, etc.

Our analysis has been based on the interpretation of the physical chemistry of the measurements. However, the overall research must bear in mind the practical ends of the problem. For example, it is known that the  $\text{pH}$  of a healthy vagina is in the range  $\text{pH}$  4–6 and that the  $\text{pH}$  of semen is in the range  $\text{pH}$  6–8. The current study seems to suggest that the H9 cell surface, which is permissive for HIV-1 replication, is zwitterionic. In general, the surface is maximally negatively charged in alkaline conditions as might be experienced in the presence of semen. The surface is positively charged under certain (fairly acidic) conditions that might be encountered in the vagina. The actual degree of surface charge is also dependent upon the prevailing conductivity of the vaginal fluids. This suggests that the best candidate for a microbicide active needs, itself, to be zwitterionic so as to be able to mirror-image the shift in sign of surface charge as the  $\text{pH}$  of the vaginal tract changes. In addition, the formulation of the topical microbicide might need to include a swamping concentration of electrolyte, to provide a conductivity in excess of that found in vaginal fluids, to eliminate any potential shifts in IEP.

**Acknowledgment.** We are grateful for the extensive contributions of Mr. Frasier McNeil-Watson (Malvern Instruments UK Ltd.) for his continued support in software development and data manipulation. Financial support has been provided by the International Partnership for Microbicides, Silver Spring, Maryland.

LA050619K